Structure of the intersection space associated with *Z*/*E* photoisomerization of retinal in rhodopsin proteins

Annapaola Migani, Adalgisa Sinicropi, Nicolas Ferré, Alessandro Cembran, Marco Garavelli and Massimo Olivucci*

Dipartimento di Chimica, Università di Siena, Via Aldo Moro, I-53100 Siena, Italy

Received 24th November 2003, Accepted 13th February 2004
First published as an Advance Article on the web 14th May 2004

In this paper we employ a CASSCF/AMBER quantum-mechanics/molecular-mechanics tool to map the intersection space (IS) of a protein. In particular, we provide evidence that the S_1 excited-state potential-energy surface of the visual photoreceptor rhodopsin is spanned by an IS segment located right at the bottom of the surface. Analysis of the molecular structures of the protein chromophore (a protonated Schiff base of retinal) along IS reveals a type of geometrical deformation not observed *in vacuo*. *Such a structure suggests that conical intersections mediating different photochemical reactions reside along the same intersection space*. This conjecture is investigated by mapping the intersection space of the rhodopsin chromophore model 2-*Z*-hepta-2,4,6-trieniminium cation and of the conjugated hydrocarbon 3-*Z*-deca-1,3,5,6,7-pentaene.

1. Introduction

The computational investigation of a photochemical reaction requires the characterization of the associated photochemical funnel.[1,2] This is defined as the point of the excited-state reaction path where the reactant decays to the ground state and prompts photoproduct formation. In many singlet reactions the funnel corresponds to a conical intersection (CI) between the excited- (S_1) and ground- (S_0) state energy surfaces.[1] CIs are not isolated points of the *n*-dimensional potential-energy surface (*n* is the number of vibrational degrees of freedom of the system) but belong to a maximally $n-2$ dimensional set of intersection points called intersection space[3] or seam of intersection[4] (IS).

In the past methods have been developed to compute conical intersection structures using energy criteria.[5,6] Indeed, the lowest-energy point of IS has been often taken as a model of the photochemical funnel. However the mapping of different S_1 reaction paths has shown that, in several cases, such paths do not end up at the lowest-energy point of the S_1/S_0 IS but at a structurally and energetically different conical intersection point.[7–9] This suggests that the mapping of the (lowest-lying) segments of IS for different classes of chromophores and reactions could be a potentially important target in computational photochemistry.

There is a second motivation for a systematic investigation of the IS structure. This concerns the fact that, for a specific organic chromophore, one may often determine different low-lying S_1/S_0 CIs each one driving a different chemical reaction.[10–18] It is not clear if these CIs belong to different IS segments or are part of the same extended IS. In other words one wants to know if a certain set of different photochemical funnels are topologically isolated. While this question may appear of purely theoretical interest, in the following we provide evidence that IS segments connecting

chemically distinct CIs may play a role in the "environmental" or substituent control of reaction selectivity.

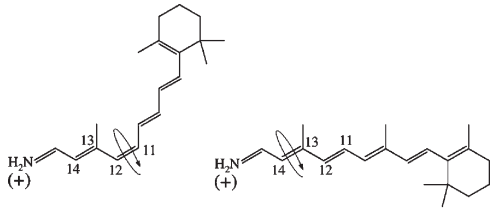

PSB11 PSBT

The photoisomerization of the retinal chromophore triggers the conformational changes underlying the activity of rhodopsin proteins.[19–22] In the visual pigment of superior animals rhodopsin (Rh)[23,24] the absorption of a photon of light causes the isomerization of the 11-*cis* isomer of the chromophore (PSB11) to its *all-trans* isomer (PSBT). Similarly, in the related bacterial proton-pump bacteriorhodopsin (bR), the photoexcitation causes the isomerization of the *all-trans* isomer (PSBT) of the same chromophore to its 13-*cis* isomer (PSB13). Computational work[25,26] on different isolated (*i.e. in vacuo*) models of PSB11 and PSBT has shown that upon photoexcitation the chromophore structure evolves towards a S_1/S_0 CI that provides the photochemical funnel. More recently we have also shown that, in the same models, the S_1 reaction paths driving isomerization about *different* double bonds (*e.g.* $C_{11}=C_{12}$ in PSB11 and $C_{13}=C_{14}$ in PSBT)[27–29] end at structurally *different* CI structures. In particular, each CI is characterized by a large twisting deformation (around 90°) about the isomerizing bond with the other bonds fully untwisted (*ca.* 0° or 180°). As mentioned above, it is presently not known if these chemically different CIs belong to the same IS.

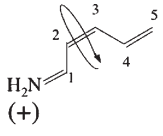

2-*Z*-penta-2,4-dieniminium cation

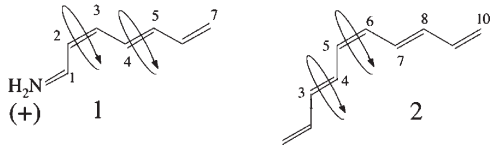

Extensive or limited mapping of IS segments of tri- and tetra-systems[30] as well as of a few organic chromophores[9,18,30–33] has been previously reported. Recently we have reported,[9] the mapping of a low-lying IS segment of the 2-*Z*-penta-2,4-dieniminium cation, a minimal model of PSB11. The data show that such a segment, located at the very bottom of the S_1 potential-energy surface, is geometrically characterized by a large change (from *ca.* 70° to *ca.* 92°)[34] of the C_1–C_2–C_3–C_4 torsional angle suggesting that its points drive the same (2-*Z* → 2-*E*) chemical event. This result suggests that a similar feature may exist at the bottom of the S_1 energy surface of Rh. In other words, it indicates that an extended low-lying IS segment may exist in native protein photoreceptors.

While scattered sets of conical intersection points obtained *via* semi-empirical[35,36] and *ab initio*[37] trajectory computations have been reported for rhodopsins, the IS structure associated with a photoisomerization reaction *in a protein environment* has, to our knowledge, never been investigated. Below we show that using the "brute-force" CASSCF/AMBER quantum-mechanics/molecular-mechanics (QM/MM) strategy developed in our lab[38] we have successfully mapped the IS segment located right at the bottom of the S_1 energy surface of both Rh and (partially) bR. The analysis of these results indicates that photochemical funnels mediating competing *Z*/*E* photoisomerizations of the retinal chromophore, reside in the *same* IS. This conjecture is investigated by

extensive mapping of the S_1/S_0 IS of the retinal chromophore model 2-*Z*-hepta-2,4,6-trieniminium cation **1** where two structurally different conical intersections, mediating the 2-*Z* → 2-*E* and 4-*E* → 4-*Z* photoisomerizations, respectively, are shown to reside in the same IS segment.

The validity of the idea that different regions of the same IS mediate production of different isomeric products is further generalized by showing that the 5-*Z*-deca-1,3,5,6,7-pentaene hydrocarbon **2**, a substantially different chromophore, displays similar features.

2. Computational methods

2.1 CASSCF/AMBER computations

While a number of QM/MM studies have been reported[39] for rhodopsin proteins, only a few employed *ab initio* QM techniques. Yamada *et al.*[40] used a RHF/6-31G/AMBER scheme to investigate the ground-state stability of the PSB11 protonated state in Rh. Hayashi *et al.*[41] reported a CASSCF//HF/DZV/AMBER computation of the λ_{max} of the related pigment bR. More recently a MD simulation of the photoisomerization of bR has been reported by Hayashi *et al.*[37] that have used a CASSCF/AMBER force field with a CASSCF truncated active space (6 electrons in 6 π-orbitals).

The *ab initio* QM/MM scheme used in this work is described in ref. 38. Briefly, the method is based on a carefully parameterized hydrogen link-atom scheme[42,43] with the frontier placed at the C_δ–C_ε bond of the Lys296 side chain in Rh (see Scheme 1a) and Lys216 in bR (see Scheme 1b). The QM calculations are based on a CASSCF/6-31G* level including an active space that comprises the full (12 electrons in 12 orbitals) π-system of PSB11 and PSBT. The MM (we use the AMBER force field) and QM segments interact in the following way: (i) the QM electrons and the full set of MM point charges interact *via* the one-electron operator, (ii) stretching, bending and torsional[43] potentials involving at least one MM atom are described by the MM potential (iii) QM and MM atom pairs separated by more than two bonds interact *via* either standard or re-parameterized[38,43,44] van der Waals potentials. CASSCF/6-31G*/AMBER geometry optimizations are carried out with the GAUSSIAN98[45] and TINKER[46] programs.

The protein framework used in the Rh computations (see also ref. 38) is derived from monomer A deposited in the PDB archive as file 1HZX.[47] With the exception of the Glu113 counterion (forming a salt-bridge with NH(+)) the Rh cavity is set neutral consistently with the experiment.[48]

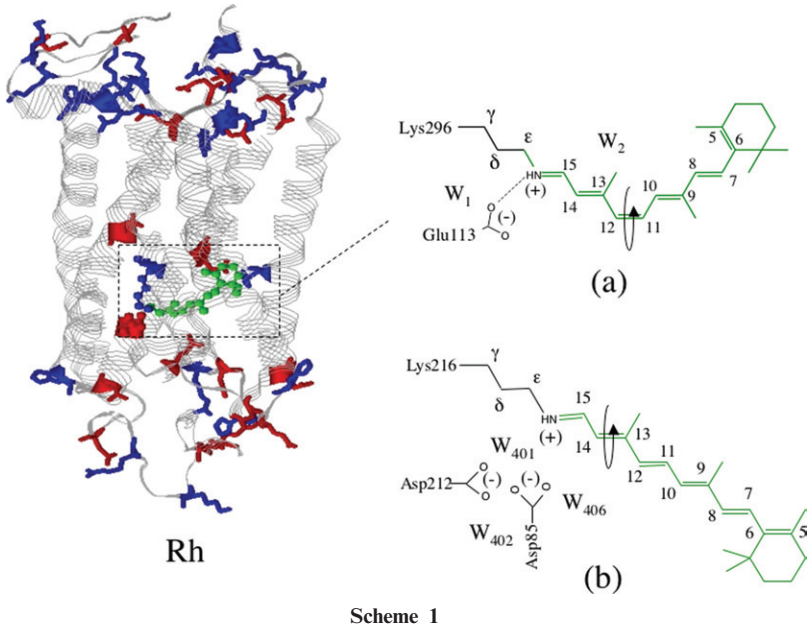

Scheme 1

While the protein is kept frozen during the optimization, the Lys296 side chain, the position/orientation of two TIP3P water molecules (W_1 and W_2 in the Scheme 1a above) and the chromophore are relaxed.[49] The AMBER charges account for S_0 polarization effects in a mean-field way.[50] The same charges are used for the excited-state computations with no *ad hoc* dielectric constant. The protein framework used in the bR computations is derived from the PDB file 1C3W,[51] with the addition of the Thr157-Glu161 missing loop taken from the 1QM8[52] file.[53] According to experimental[54,55] and previous theoretical[41,56,57] works, we set the protonation state of Asp96, Asp115 and Glu204 neutral, while for all the other residues we use the standard protonation states. The resulting (+3) overall charge is neutralized placing three chloride ions on the protein surface (one near Arg171, another in proximity of Arg221, Arg223 and Lys26 and the other near Lys125). The position of the three water molecules W_{401}, W_{402} and W_{406} (see Scheme 1b above) is optimized at the HF/6-31G* level, and kept frozen during all the following chromophore geometry optimizations (the Lys296 side chain and the chromophore are free to relax, as for Rh).

2.2 Intersection space mapping

The mapping of the *lowest-lying* IS segment of Rh and bR has been carried out using standard constrained geometry optimizations. The constraint is defined by fixing the C_{11}–C_{12} torsional angle at the values of 70°, 80°, 90°, 100°, and 110° for Rh, and the C_{13}–C_{14} torsional angle at the values of 90°, 100°, and 110° for bR. The use of standard geometry optimizations is possible because in these systems the IS spans the region of the absolute minima of the S_1 potential-energy surface (in all cases the optimization is stopped when the S_1 CASSCF energy value does not further improve for at least two successive optimization steps or fails to converge due to root flipping).

For structures **1** and **2** two low-lying one-dimensional cross-sections (*i.e.* segments) of IS were computed according to the following procedure. (i) For each species two conical intersection points mediating alternative photoisomerization processes (*i.e.* the 2-*Z* → 2-*E* and 4-*E* → 4-*Z* conversions in **1** and 3-*E* → 3-*Z* and 5-*Z* → 5-*E* in **2**) are determined *via* standard unconstrained conical intersection optimization (CIO) using the methodology available in GAUSSIAN98.[45,58] These conical intersection points are local "minima" on the IS. (ii) For each species a tentative low-lying IS "transition structure" is determined with the same CIO method by imposing one or more geometrical constraints during the optimization (see Sections 3.2 and 3.3). Such constraints are chosen on the basis of the chemical intuition. (iii) Each optimized tentative IS "transition structure" is rigorously connected to the two local IS minima *via* computation of two *steepest-descent paths within the IS* (ISDP). This strategy can be described as a combination of the intrinsic relaxation direction (IRD) method for finding local steepest-descent directions from a non-stationary point[59] and CIO method for locating conical intersections as energy minima within the intersection space.[58] A full description of the ISDP method is given in ref. 32.

3. Results and discussion

3.1 The intersection space of Rh (and bR)

In this section we report the *first* attempt to map the lowest-lying (one dimensional) IS segment in photoreceptor proteins. The model used in the Rh computations is illustrated in Scheme 1a where the part treated at the CASSCF level (*i.e.* the PSB11 chromophore) is given in green. The fact that only the structure of PSB11, the entire Lys296 side chain and the position of two water molecules W_1 and W_2 are fully optimized during the conical intersection search may appear a crude approximation. However it is known that this region of the S_1 potential-energy surface of the protein is reached in less than 50 fs and left after *ca.* 150 fs.[23,24] Such a time scale is not consistent with significant distortion of the S_0 equilibrium structure of the protein backbone and cavity residues.

The computed IS energy profile of Rh is reported in Fig. 1. In the same figure we report the structural changes characterizing the IS coordinate (only the relevant moiety of PSB11 is shown). From inspection of these data, it is apparent that such a coordinate is dominated by the torsional mode describing the PSB11 → PSBT isomerization. Indeed the IS develops along a flat energy

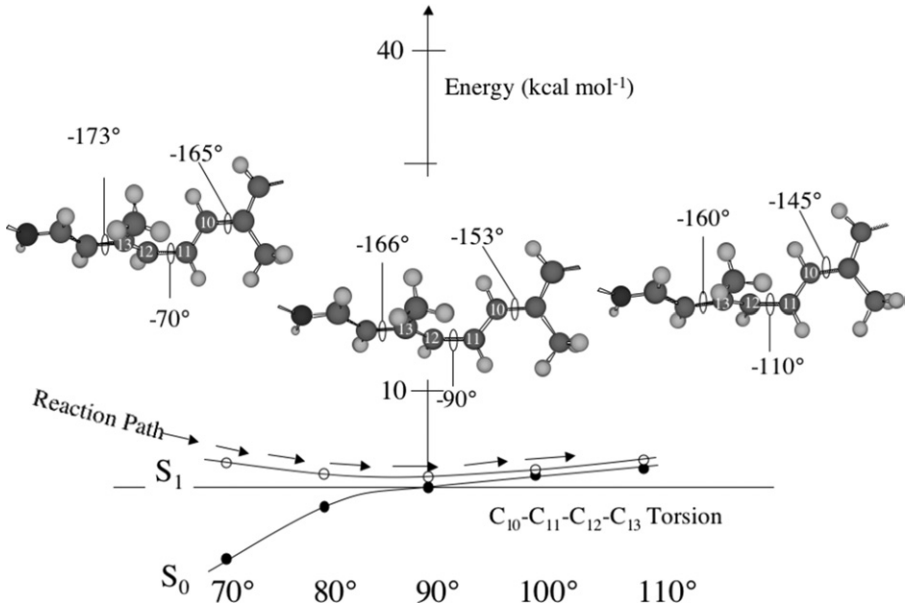

Fig. 1 CASSCF/AMBER energy profile and relevant geometrical changes along the "Reaction Path" segment located at the bottom of the S_1 state of Rh. The path is obtained by fixing the value of the C_{10}–C_{11}–C_{12}–C_{13} dihedral during the S_1 CASSCF/AMBER optimization.

plateau characterized by a 80°–110° change in the C_{10}–C_{11}–C_{12}–C_{13} torsion with the 90° twisted intersection point corresponding both to the lowest-energy IS point and S_1 absolute energy minimum.

The absolute and relative energies of Rh, **1** and **2** are listed in Table 1.

The idea that the PSB11 → PSBT isomerization coordinate develops along an IS segment and not, as usually assumed,[23,24] orthogonally to it, is demonstrated by the branching plane vectors ($\boldsymbol{X}_1$ and $\boldsymbol{X}_2$) computed at the 90° point. Neither of the two vectors corresponds to a C_{10}–C_{11}–C_{12}–C_{13} torsional mode. Indeed, as shown in Fig. 2, the branching plane is characterized by the combination of a stretching mode (a coupled double-bond expansion and single-bond compression mode) and a coupled wagging mode[60] (simultaneous pyramidalization at the C_{10} and C_{13} centers) of the PSB11 skeleton. In summary, the local shape of the bottom of the S_1 energy surface can be represented by the schematic illustration of Scheme 2.

Taking into account the results mentioned in the introduction, such an IS feature seems to be a consequence of the protonated Schiff base nature of the chromophore and not a consequence of the protein environment. In fact, the same feature has been documented[9] for a minimal PSB11 chromophore model *in vacuo*. The similarity of the CIs of Rh and the CIs of an isolated (*in vacuo*) protonated Schiff base is also indicated by the close shape of the branching space vectors of PSB11 in Rh and compound **1** (see Fig. 2).

All reported *in vacuo* models of PSB11 or PSBT display low-lying (usually *ca.* 90° twisted) CIs characterized by a structure with only *one* twisted bond. Even when two chemically distinct conical intersection minima are found[28] (*e.g.* conical intersections driving different isomerization processes), these show, invariably, two 90° twisted planar moieties. One of these cases is reported in Scheme 3 for the chromophore model **1** featuring the conical intersections T,*E*-**1**-CI and *Z*,T-**1**-CI (where "T" stands for "twisted") driving the isomerization of the C_2–C_3 and C_4–C_5 double bonds, respectively. In contrast with this and the other models, the lowest-energy (90° twisted) conical intersection found in Rh (see Fig. 1) is not only twisted about the reactive C_{11}–C_{12} bonds but also about the *two* adjacent (*i.e.* C_9–C_{10} and C_{13}–C_{14}) double bonds (notice that these torsional deformations increase along the IS). This suggests that low-lying conical intersection points can also be found for structures where different double bonds are, simultaneously, partially or totally twisted.

Table 1 CASSCF 6-31G*/AMBER (Rh and bR) and CASSCF 6-31G* (**1** and **2**) absolute (E) and relative (ΔE) energies

Structure	State	E/E_h	ΔE/kcal mol^{-1}
Rhodopsin proteins			
Rh (90°)[c]	S_0	−868.48640	−1.07
	S_1	−868.48469	0.00[a]
bR (90°)[c]	S_0	−869.82311	−0.15
	S_1	−869.82287	0.00[b]
2-*Z*-hepta-2,4,6-trieniminium cation (**1**)			
E,E-**1**-FC[f]	S_0	(−325.18633)	—
	S_0	−325.17504[e]	−93.56
	S_1	−325.02594[e]	0.00[d]
T,*E*-**1**-CI[f]	S_0	−325.08140	−34.80
	S_1	−325.08130	−34.74
E,T-1-CI[f]	S_0	−325.07535	−31.01
	S_1	−325.07522	−30.92
Z,T-**1**-CI[f]	S_0	−325.07232	−29.11
	S_1	−325.07188	−28.83
T,*Z*-**1**-CI[f]	S_0	−325.07788	−32.59
	S_1	−325.07785	−32.57
T,T-**1**-CI[f]	S_0	−325.05303	−17.00
	S_1	−325.05236	−16.58
5-*Z*-deca-1,3,5,6,7-pentaene (**2**)			
2-FC	S_0	(−385.72061)	—
	S_0	−385.71706[e]	−104.34
	S_1	−385.55079[e]	0.00[g]
T,τ-**2**-CI[c]	S_0	−385.56093	−6.60
	S_1	−385.56131	−6.36
T,τ,T-**2**-CI[c]	S_0	−385.54786	1.84
	S_1	−385.54771	1.93
τ,T-**2**-CI[c]	S_0	−385.55517	−2.75
	S_1	−385.55523	−2.79

[a] Energies relative to the Rh (90°) S_1 state. [b] Energies relative to the bR (90°) S_1 state. [c] Geometry optimized with state-average (weights 0.5, 0.5) CASSCF wave function. [d] Energies relative to the *E,E*-**1** isomer. [e] S_0, S_1 state-average energies (weights 0.5, 0.5) at the single-root optimized ground state minimum (S_0 energy in parenthesis). [f] Geometry optimized with state-average (weights 0.5, 0.5) CASSCF wave function. The gradient was corrected with the CP-MC-SCF correction. [g] Energies relative to the isomer **2**.

Since, geometrically, these multiply twisted CIs are intermediate between different singly twisted CIs one may suggest that a continuum (*i.e.* an IS segment) of such CIs exists that connects two singly twisted (and chemically distinct) CIs. A corollary of this hypothesis is that, in general, the effect of the cavity of Rh proteins would be that of stabilizing or destabilizing specific regions of the extended IS space of the retinal chromophore. In other words, the stabilization of the IS region leading to C_{11}–C_{12} double bond isomerization and destabilization of the regions controlling the C_{13}–C_{14} or C_9–C_{10} double bonds may be one factor contributing to the isomerization selectivity observed in Rh.

The hypothesis reported above is also in line with the fact that, as already mentioned in the introduction, the retinal chromophore of the bacterial photoreceptor bR undergoes selective isomerization about the C_{13}–C_{14} double bond. The preliminary results of the IS mapping of bR are reported in Fig. 3. In contrast to Rh, the lowest-lying point of the IS segment of Fig. 3 does not correspond to a conical intersection with a 90° twisted double bond. In fact a lower intersection point could be located that features a *ca.* 110° C_{15}–C_{14}–C_{13}–C_{12} torsional angle and lies *ca.* 6 kcal mol^{-1} below the 92° twisted conical intersection. (We are currently investigating the possibility that this IS segment comprises C_{15}–C_{14}–C_{13}–C_{12} dihedral angles larger than 110°.) The fact that the lowest-lying IS segment displays a highly twisted C_{13}–C_{14} double bond indeed suggests that the specific shape of the protein cavity stabilizes the IS region dominated by a highly twisted C_{13}–C_{14}

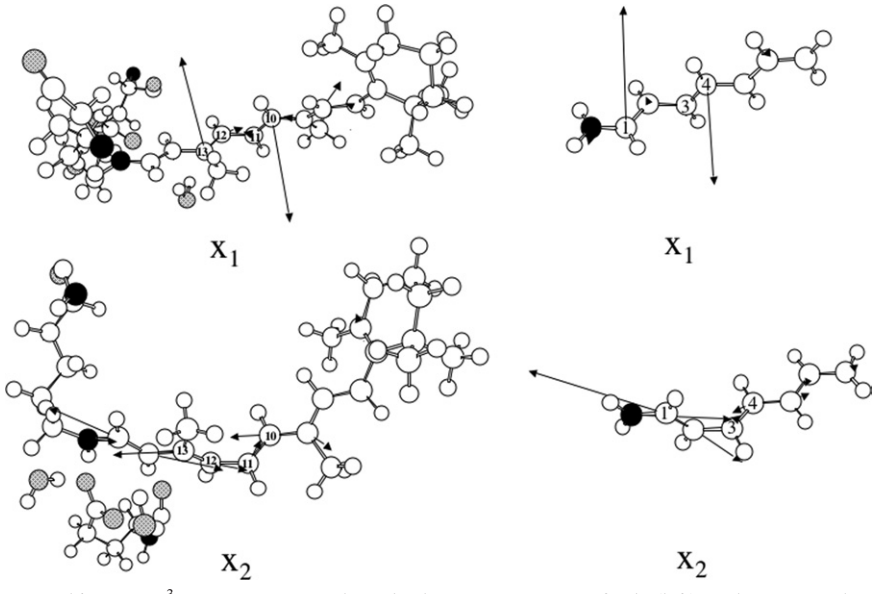

Fig. 2 Branching space[3] vectors computed at the lowest-energy CI of Rh (left) and compound **1** (right). Vector $\boldsymbol{X}_1$ corresponds to the gradient difference while $\boldsymbol{X}_2$ corresponds to the derivative coupling.

rather than C_{11}–C_{12} double bond. Notice also that while the protein environment may change the character of the lowest-lying segment of the IS, the branching space vectors (see Fig. 3) maintain the same shape seen in Rh even if the wagging motion regards a different set of chromophore centers (*i.e.* C_{15} and C_{12} rather than C_{13} and C_{10}).

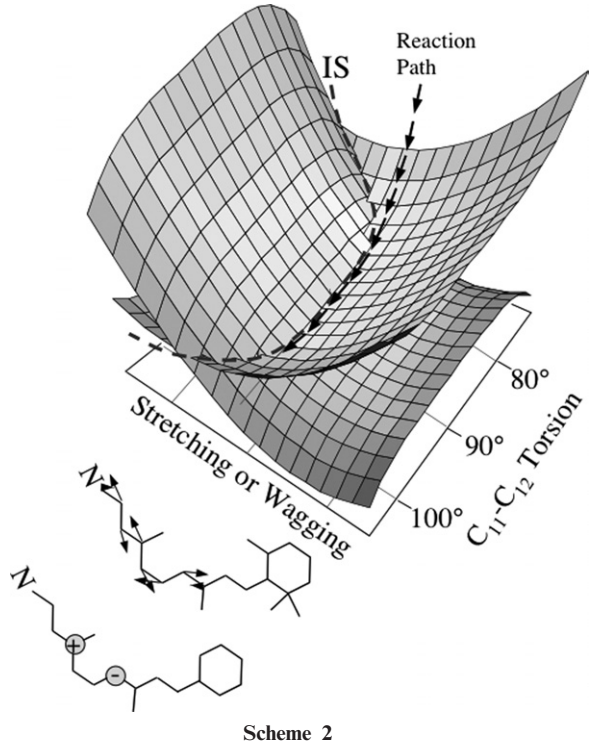

Scheme 2

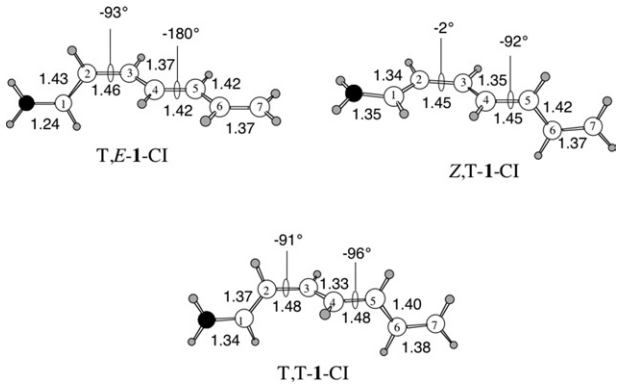

Scheme 3

3.2 The intersection space of the hepta-2,4,6-trieniminium cation

The fact that the structure of certain protonated Schiff base CIs features a combination of different twisted double bonds is suggestive of an IS space structure far more complex than the one investigated in the past. Indeed, one can foresee a situation where *singly*-twisted CIs, such as T,*E*-**1**-CI and *Z*,T-**1**-CI in Scheme 3, are connected by a *continuous segment* of (partially or totally) doubly-twisted conical intersections.

In Fig. 4 we report the results of the mapping of a low-lying IS segment of **1**. The mapping has been carried out in two steps. First, using suitable geometrical constraints (see also Section 2), we optimized a conical intersection point (T,T-**1**-CI in Scheme 3) that, tentatively, represents a "transition structure" between T,*E*-**1**-CI and *Z*,T-**1**-CI. T,T-**1**-CI is characterized by *ca.* 90° twisted C_2–C_3 and C_4–C_5 double bonds. Second, we carried out two ISDP computations starting at T,T-**1**-CI and pointing to T,*E*-**1**-CI and *Z*,T-**1**-CI, respectively. As shown in Fig. 4a the results demonstrate that the three conical intersections belong to the same IS segment. From the analysis

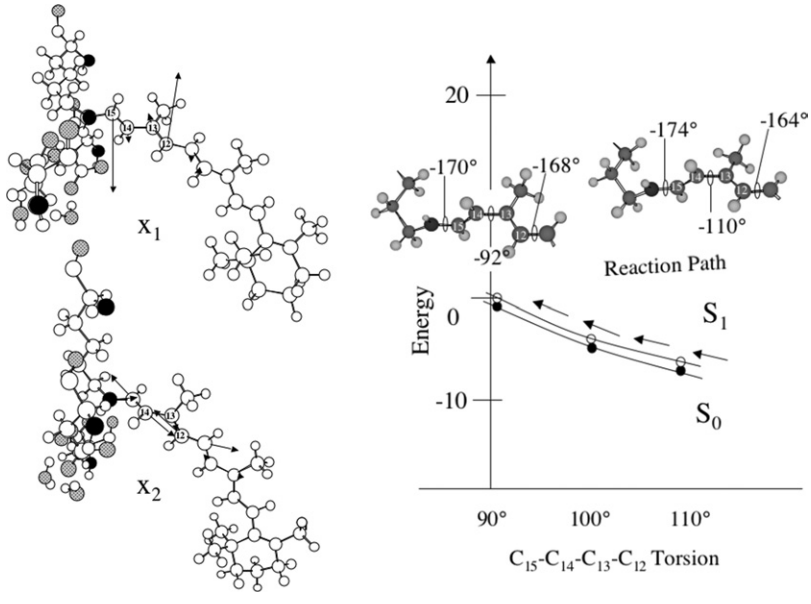

Fig. 3 Branching space vectors (left) and CASSCF/Amber energy profile (right) along the *initial part* of the "Reaction Path" segment located at the bottom of the S_1 state of bR.

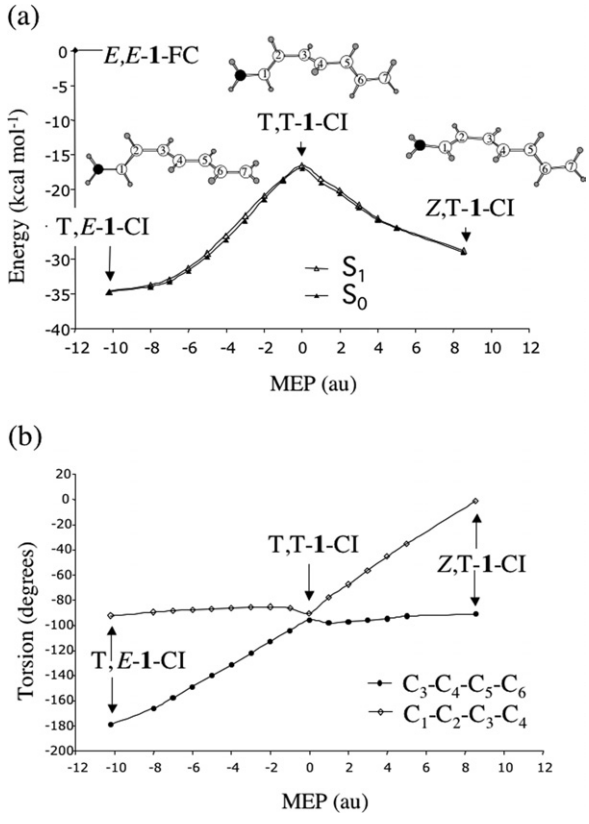

Fig. 4 (a) CASSCF energy profile along the IS coordinate connecting the chemically distinct CI minima T,*E*-**1**-CI and *Z*,T-**1**-CI. The energy values are relative to the (most stable) *E,E*-**1** isomer (the nomenclature adopted refers to the $-C_2-C_3-C_4-C_5-$ fragment). (b) IS coordinate analysis along the corresponding path.

of the T,*E*-**1**-CI ↔ T,T-**1**-CI ↔ *Z*,T-**1**-CI coordinate (see Fig. 4b) it is apparent that one can smoothly change the amount of twisting about the C_2–C_3 and C_4–C_5 bonds without leaving the IS. Thus, in principle, certain substituents or a suitably designed molecular environment can change the energy profile of Fig. 4a favoring one isomerization channel over the other or even stabilizing the central part of it.

Starting at the same T,T-**1**-CI structure it is also possible to compute two additional paths that connect this point to the *E*,T-**1**-CI and T,*Z*-**1**-CI singly-twisted conical intersections, respectively. This finding demonstrates that T,T-**1**-CI (*i.e.* the top structure) is better interpreted as a local maximum (actually a saddle point of index 2) on IS and not as a "transition state". In Fig. 5 we show that a 3D plot of the four ISDPs suggests the existence of a low-lying two-dimensional cross-section (*i.e.* a surface) of the IS space spanned by CI structures characterized by different degrees of twisting of the two central bonds. As schematically indicated in the diagram on the right side of the figure, this information also suggests the existence of four IS transition structures connecting the four IS minima along a "circle".

3.3 The intersection space of deca-1,3,5,6,7-pentaene

Above we have shown that in protonated Schiff bases CIs mediating different isomerization events belong to the same IS. In this subsection we demonstrate that this result can be extended to chromophores characterized by excited states of different nature and displaying CIs with a totally different geometrical structure. In fact, while the S_1 state of **1** has a net ionic (*i.e.* charge-transfer) character, the conjugated hydrocarbon **2** has a lowest-lying singlet excited state with a covalent

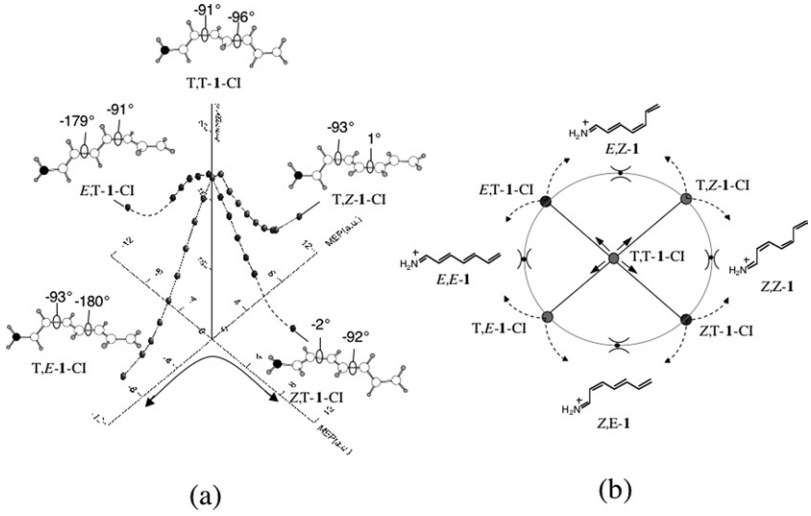

Fig. 5 (a) 3D representation of the IS steepest descent paths (ISDPs) connecting T,T-**1**-CI to the four IS local minima of compound **1**. (b) Schematic 2D representation of the topology of the IS surface in this region. Notice the hypothetical presence of four IS transition structures connecting the local minima. The potential photoproducts (*E*,*Z*-**1**, *Z*,*E*-**1** *Z*,*Z*-**1** and *E*,*E*-**1**) of decay at each minimum are also given. The curved arrow marks the T,*E*-**1**-CI ↔ T,T-**1**-CI ↔ *Z*,T-**1**-CI profile shown in Fig. 4a.

(*i.e.* diradical) character.[61–65] Furthermore the local CI minima of **2** are characterized by a rather complex deformation corresponding to a polymethine $-(CH)_3-$ kink along the hydrocarbon chain.[66] These can also be described in terms of doubly-twisted structures about one double bond and one of its adjacent single bonds. The involvement of these types of CIs in both the *Z*/*E* isomerization and ultrafast $S_1 \rightarrow S_0$ radiationless relaxation of linear and cyclic polyenes has been reported.[10,67,68]

As shown in Fig. 6, one can locate two conical intersection minima (T,τ-**2**-CI and τ,T-**2**-CI) where the $-(CH)_3-$ kink spans the $-C_3-C_4-C_5-$ moiety and the $-C_4-C_5-C_6-$ moieties respectively (here uppercase "T" indicates twisted double bonds and lowercase "τ" indicates twisted single bonds). In this case the tentative "transition structure" connecting the two local IS minima has been computed by imposing a geometrical constraint (103° and 112° constrained values for the $-C_3-C_4-C_5-$ and $-C_4-C_5-C_6-$ angles, respectively) during the conical intersection optimization. The optimized structure (T,τ,T-**2**-CI) reported in Fig. 6 displays a different and more extended type of kink (*i.e.* a $-(CH)_4-$ kink along the $-C_3-C_4-C_5-C_6-$ moiety) involving four rather than three carbon atoms of the chain. ISDP computations demonstrate that, similar to protonated Schiff bases, the three CI structures belong to the same IS.

While the results reported above demonstrate that IS segments containing chemically different CIs exist in chromophores with different excited states, such an investigation was limited to isomerization reactions. In other words in both **1** and **2** the chemical event mediated by the IS points involves exclusively π-bond breaking and making. Thus, in order to further generalize our findings we report in Fig. 7 a preliminary result concerning the photocyclization of **2**. Accordingly, in the figure we report the optimized structure of two CIs (cyclohepta-CI and cyclonona-CI) that mediate different types of cyclization. In fact, the 6-vinyl,7-methylene-cyclohepta-1,3-diene-like and 8-methylene-cyclonona-1,3,5-triene-like structures of the two S_1/S_0 CIs are consistent with production, upon decay to the ground state, of the corresponding S_0 diradicals. These are the potential intermediates involved in the production of the corresponding 6-vinyl-bicyclo[5.1.0]octa-2,4-diene and bicyclo[7.1.0]deca-2,4,6-triene photoproducts. Remarkably we have been able to locate a 9-methylene-bicyclo[5.2.0]nona-2,4-diene-like conical intersection (TS in Fig. 7) that is structurally intermediate between the two minima and that therefore represents a tentative transition state on IS. Further work is needed to rigorously demonstrate that these three conical intersections belong to the same IS.

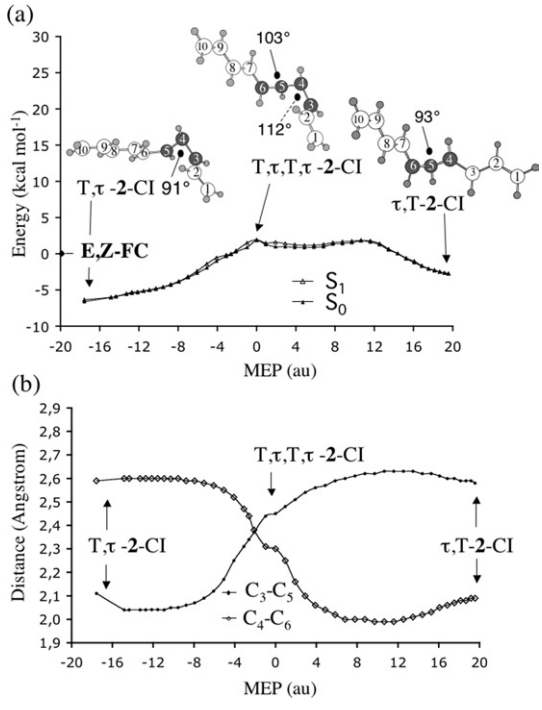

Fig. 6 (a) CASSCF energy profile along the IS coordinate connecting the chemically distinct CI minima T, τ-**2**-CI and τ,T-**2**-CI (the T and τ refer to the three bonds of the $–C_3–C_4–C_5–C_6–$ fragment). The energy values are relative to isomer **2**. The energy plateau spanning the 0–12 E_h coordinate range is associated with a *ca.* 80° torsional deformation about the $C_4–C_3$ bond. (b) IS coordinate analysis along the corresponding path.

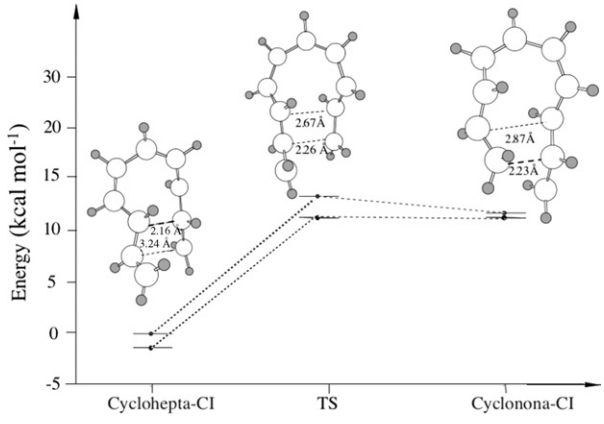

Fig. 7 Possible CASSCF/STO-3G energy profile along the IS coordinate connecting two CI minima of **2** (cyclohepta-CI and cyclonona-CI) mediating distinct photocyclizations.

4. Conclusions

In general a conical intersection acts as a very efficient non-adiabatic $S_1 \rightarrow S_0$ decay channel prompting ground state relaxation. For this reason the lowest-energy CI point of PSB11 (displaying a *ca.* 90° $C_{10}–C_{11}–C_{12}–C_{13}$ torsion) has been often taken as a model of the "photochemical

funnel" of Rh. Above we have shown that this model may be incomplete. This is due to the fact that the bottom of the S_1 energy surface of Rh is spanned by a fairly extended IS segment displaying values of the C_{10}–C_{11}–C_{12}–C_{13} torsion going from 80° to 110°. It is thus clear that a correct non-adiabatic semi-classical or quantum dynamics simulation based on an analytical representation of the S_1 energy surface must include the full IS segment.

The fact that in different organic chromophores there are low-lying IS segments featuring regions controlling distinct chemical reactions, suggests that the knowledge of the detailed topology of the $n-2$ dimensional IS is of importance for the comprehension of substituent or catalytic effects or, more generally, of the photochemical reactivity. Regrettably, efficient and rigorous computational tools for the optimization of, for instance, transition structures and saddle points within the IS are still not available. Accordingly, we believe that the formulation and implementation in a quantum chemical code of such tools will constitute a step forward in the field of computational photochemistry.

Acknowledgements

Funds have been provided by the Università di Siena (Progetto di Ateneo 02/04) and HFSP (RG 0229/2000-M). N.F. is grateful for the EU grant HPMF-CT-2001-01769. We thank CINECA for granted calculation time.

References

1 F. Bernardi, M. Olivucci and M. A. Robb, *Chem. Soc. Rev.*, 1996, **25**, 321.
2 F. Bernardi, M. Olivucci, J. Michl and M. A. Robb, in *The Spectrum*, 1996, Bowling Green State University, Bowling Green, OH, vol. 9, p. 1.
3 G. J. Atchity, S. S. Xantheas and K. Ruedenberg, *J. Chem. Phys.*, 1991, **95**, 1862.
4 D. R. Yarkony, *J. Phys. Chem. A*, 2001, **105**, 6277.
5 M. A. Robb, M. Garavelli, M. Olivucci and F. Bernardi, *Reviews in Computational Chemistry*, ed. K. B. Lipkowitz, D. B. Boyd, New York, Chichester, 2000, vol. 15, 87–146.
6 D. R. Yarkony, *J. Phys. Chem.*, 1993, **97**, 4407.
7 M. Boggio-Pasqua, M. J. Bearpark, P. A. Hunt and M. A. Robb, *J. Am. Chem. Soc.*, 2002, **124**, 1456.
8 M. Ben-Nun and T. J. Martinez, *Chem. Phys. Lett.*, 1998, **298**, 57.
9 A. Migani, M. A. Robb and M. Olivucci, *J. Am. Chem. Soc.*, 2003, **125**, 2804.
10 M. Garavelli, P. Celani, F. Bernardi, M. A. Robb and M. Olivucci, *J. Am. Chem. Soc.*, 1997, **119**, 11 487.
11 M. J. Bearpark, M. Deumal, M. A. Robb, T. Vreven, N. Yamamoto, M. Olivucci and F. Bernardi, *J. Am. Chem. Soc.*, 1997, **119**, 709.
12 M. Deumal, M. J. Bearpark, B. R. Smith, M. Olivucci, F. Bernardi and M. A. Robb, *J. Org. Chem.*, 1998, **63**, 4594.
13 S. Clifford, M. J. Bearpark, F. Bernardi, M. Olivucci, M. A. Robb and B. R. Smith, *J. Am. Chem. Soc.*, 1996, **118**, 7353.
14 M. Garavelli, F. Bernardi, A. Cembran, O. Castano, L. M. Frutos, M. Merchan and M. Olivucci, *J. Am. Chem. Soc.*, 2002, **124**, 13 770.
15 I. Ohmine, *J. Chem. Phys.*, 1985, **83**, 2348.
16 M. Ben-Nun and T. J. Martinez, *Chem. Phys.*, 2000, **259**, 237.
17 L. Freund and M. Klessinger, *Int. J. Quantum Chem.*, 1998, **70**, 1023.
18 S. Wilsey and K. N. Houk, *J. Am. Chem. Soc.*, 2002, **124**, 11 182.
19 T. Yoshizawa and O. Kuwata, in *CRC Handbook of Organic Photochemistry and Photobiology*, ed. W. M. Horspool and P.-S. Song, CRC, Boca Raton, FL, 1995.
20 G. Wald, *Science*, 1968, **162**, 230.
21 M. Ottolenghi and M. Sheves, *Isr. J. Chem.*, 1995, **35**, 193.
22 R. Needleman, in *CRC Handbook of Organic Photochemistry and Photobiology*, ed. W. M. Horspool and P.-S. Song, 1995.
23 H. Kandori, Y. Shichida and T. Yoshizawa, *Biochemistry (Moscow)*, 2001, **66**, 1483.
24 R. A. Mathies and J. Lugtenburg, in *Handbook of Biological Physics*, ed. D. G. Stavenga, W. J. d. Grip and E. N. Pugh, 2000.
25 R. Gonzalez-Luque, M. Garavelli, F. Bernardi, M. Merchan, M. A. Robb and M. Olivucci, *Proc. Natl. Acad. Sci. USA*, 2000, **97**, 9379.
26 A. Sinicropi, A. Migani, L. De Vico and M. Olivucci, *Photochem. Photobiol.Sci.*, 2003, **2**, 1250.
27 M. Ben-Nun, F. Molnar, K. Schulten and T. J. Martinez, *Proc. Natl. Acad. Sci. USA*, 2002, **99**, 1769.
28 L. De Vico, C. S. Page, M. Garavelli, F. Bernardi, R. Basosi and M. Olivucci, *J. Am. Chem. Soc.*, 2002, **124**, 4124.

29 M. Garavelli, F. Bernardi, M. Olivucci, T. Vreven, S. Klein, P. Celani and M. A. Robb, *Faraday Discuss.*, 1998, **110**, 51.
30 D. R. Yarkony, *J. Phys. Chem. A*, 1999, **103**, 6658.
31 M. Ben-Nun and T. J. Martinez, *Chem. Phys.*, 2000, **259**, 237.
32 M. Garavelli, C. S. Page, P. Celani, M. Olivucci, W. E. Schmidt, S. A. Trushin and W. Fuss, *J. Phys. Chem. A*, 2001, **105**, 4458.
33 D. R. Yarkony and S. Matsika, *J. Am. Chem. Soc.*, 2003, **125**, 10 672.
34 More recently we have shown that the low-lying IS segment extends beyond 92° up to 126° twisting. O. Weingart, A. Migani, M. Olivucci, M. A. Robb, V. Buß and P. Hunt, submitted.
35 A. Warshel and Z. T. Chu, *J. Phys. Chem. B*, 2001, **105**, 9857.
36 A. Warshel, Z. T. Chu and J.-K. Hwang, *Chem. Phys.*, 1991, **158**, 303.
37 S. Hayashi, E. Tajkhorshid and K. Schulten, *Biophys. J.*, 2003, **85**, 1440.
38 N. Ferré and M. Olivucci, *J. Am. Chem. Soc.*, 2003, **125**, 6868.
39 R. Rajamani and J. Gao, *J. Comput. Chem.*, 2002, **23**, 96.
40 A. Yamada, T. Kakitani, S. Yamamoto and T. Yamato, *Chem. Phys. Lett.*, 2002, **366**, 670.
41 S. Hayashi, E. Tajkhorshid and K. Schulten, *Biophys. J.*, 2002, **83**, 1281.
42 N. Ferré, A. Cembran, M. Garavelli and M. Olivucci, *Theor. Chem. Acc.*, in press.
43 N. Ferré and M. Olivucci, *J. Mol. Struct. (THEOCHEM)*, 2003, **632**, 71.
44 One torsion (C15–N–C_ε–C_δ) and the van der Waals forces of the PSB11 model (except NH+) have been re-parameterized to reproduce the CASSCF torsional energy profiles of a model of the frontier.
45 M. J. Frisch, G. W. Trucks, H. B. Schlegel, G. E. Scuseria, M. A. Robb, J. R. Cheeseman, V. G. Zakrzewski, J. A. M. Jr., R. E. Stratmann, J. C. Burant, S. Dapprich, J. M. Millam, A. D. Daniels, K. N. Kudin, M. C. Strain, O. Farkas, J. Tomasi, V. Barone, M. Cossi, R. Cammi, B. Mennucci, C. Pomelli, C. Adamo, S. Clifford, J. Ochterski, G. A. Petersson, P. Y. Ayala, Q. Cui, K. Morokuma, D. K. Malick, A. D. Rabuck, K. Raghavachari, J. B. Foresman, J. Cioslowski, J. V. Ortiz, A. G. Baboul, B. B. Stefanov, G. Liu, A. Liashenko, P. Piskorz, I. Komaromi, R. Gomperts, R. L. Martin, D. J. Fox, T. Keith, M. A. Al-Laham, C. Y. Peng, A. Nanayakkara, C. Gonzalez, M. Challacombe, P. M. W. Gill, B. Johnson, W. Chen, M. W. Wong, J. L. Andres, C. Gonzalez, M. Head-Gordon, E. S. Replogle and J. A. Pople, in *Gaussian 98*, Pittsburgh PA, 1998.
46 J. W. Ponder and F. M. Richards, *J. Comput. Chem.*, 1987, **8**, 1016.
47 D. C. Teller, T. Okada, C. A. Behnke, K. Palczewski and R. E. Stenkamp, *Biochemistry*, 2001, **40**, 7761.
48 K. Fahmy, F. Jager, M. Beck, T. A. Zvyaga, T. P. Sakmar and F. Siebert, *Proc. Nat. Acad. Sci. USA*, 1993, **90**, 10 206.
49 The optimized position of W1 differs from the one proposed by Okada *et al.* See the supporting information in ref. 38.
50 B. Besler, K. Merz and P. Kollman, *J. Comput. Chem.*, 1985, **11**, 431.
51 H. Luecke, B. Schobert, H. T. Richter, J. P. Cartailler and J. K. J. Lanyi, *J. Mol. Biol.*, 1999, **291**, 899.
52 K. Takeda, H. Sato, T. Hino, M. Kono, K. Fukuda, I. Sakurai, T. Okada and T. Kouyama, *J. Mol. Biol.*, 1998, **283**, 463.
53 We use the "All-Atoms Fit" option of the Swiss-PdbViewer tool (N. Guex and M. C. Peitsch, *Electrophoresis*, 1997, **18**, 2714, http://www.expasy.org/spdbv/, to superimpose the missing loop to the 156,162 and 163 residues, common to both sequences. The two "frontier" residues Thr157 and Glu161 and the side chain of Lys159 are then MM optimized with the Tinker3.9 package using the Amber force field to better fit the protein surface.
54 J. Sasaki, J. K. Lanyi, R. Needleman, T. Yoshizawa and A. Maeda, *Biochemistry*, 1994, **33**, 3178.
55 L. S. Brown, J. Sasaki, H. Kandori, A. Maeda, R. Needleman and J. K. Lanyi, *J. Biol. Chem.*, 1995, **270**, 27 122.
56 S. Hayashi and I. Ohmine, *J. Phys. Chem. B*, 2000, **104**, 10 678.
57 T. Vreven and K. Morokuma, *Theor. Chem. Acc.*, 2003, **109**, 125.
58 M. J. Bearpark, M. A. Robb and H. B. Schlegel, *Chem. Phys. Lett.*, 1994, **223**, 269.
59 O. Celani, M. A. Robb, M. Garavelli, F. Bernardi and M. Olivucci, *Chem. Phys. Lett.*, 1995, **243**, 1.
60 A. Migani and M. Olivucci, in *Conical Intersections and Organic Reaction Mechanisms*, ed. W. Domcke, D. R. Yarkony and H. Köppel.
61 M. O. Trulson and R. A. Mathies, *J. Phys. Chem.*, 1990, **94**, 5741.
62 R. R. Chadwick, M. Z. Zgiersky and B. S. Hudson, *J. Chem. Phys.*, 1991, **95**, 7204.
63 W. J. Buma, B. E. Kohler and K. Song, *J. Chem. Phys.*, 1991, **94**, 6367.
64 X. Ci and A. B. Myers, *J. Chem. Phys.*, 1992, **96**, 6433.
65 H. Petek, A. J. Bell, R. L. Christensen and K. Yoshihara, *J. Chem. Phys.*, 1992, **96**, 2412.
66 M. Garavelli, P. Celani, N. Yamamoto, F. Bernardi, M. A. Robb and M. Olivucci, *J. Am. Chem. Soc.*, 1996, **118**, 11 656.
67 M. Garavelli, B. R. Smith, M. J. Bearpark, F. Bernardi, M. Olivucci and M. A. Robb, *J. Am. Chem. Soc.*, 2000, **122**, 5568.
68 M. J. Bearpark, F. Bernardi, S. Clifford, M. Olivucci, M. A. Robb and T. Vreven, *Mol. Phys.*, 1996, **89**, 37.